Centennial-scale variability of sea-ice cover in the Chukchi Sea since AD 1850 based on biomarker reconstruction

Youcheng Bai, Marie-Alexandrine Sicre, Jian Ren, Bassem Jalali, Vincent Klein, Hongliang Li, Long Lin, Zhongqiang Ji, Liang Su, Qingmei Zhu, et al.

ENVIRONMENTAL RESEARCH
LETTERS

Centennial-scale variability of sea-ice cover in the Chukchi Sea since AD 1850 based on biomarker reconstruction

To cite this article before publication: Youcheng Bai *et al* 2022 *Environ. Res. Lett.* in press https://doi.org/10.1088/1748-9326/ac5f92

Centennial-scale variability of sea-ice cover in the Chukchi Sea since AD 1850 based on biomarker reconstruction

Youcheng Bai[a,b,c], Marie-Alexandrine Sicre[d], Jian Ren[a,b], Bassem Jalali[a,b], Vincent Klein[d], Hongliang Li[a,b], Long Lin[e], Zhongqiang Ji[a,b], Liang Su[a,f], Qingmei Zhu[g], Haiyan Jin[a,b,h], Jianfang Chen[a,b,h*]

[a]*Key Laboratory of Marine Ecosystem Dynamics, Ministry of Natural Resources, Hangzhou ,310012, China*

[b]*Second Institute of Oceanography, Ministry of Natural Resources, Hangzhou, 310012, China*

[c]*Southern Marine Science and Engineering Guangdong Laboratory (Zhuhai), Zhuhai, 519000, China*

[d]*Sorbonne Université, Pierre et Marie Curie -CNRS, LOCEAN, Case 100, 4 place Jussieu, F-75005 Paris, France*

[e]*Key Laboratory of Polar Science, MNR, Polar Research Institute of China, Shanghai, 200316, China*

[f]*Ocean College, Zhejiang University, Zhoushan,316021, China*

[g]*College of Ocean and Meteorology, Guangdong Ocean University, Zhanjiang, 524088, China*

[h]*State Key Laboratory of Satellite Ocean Environment Dynamics, Second Institute of Oceanography, Ministry of Natural Resources, Hangzhou ,310012, China*

[*] Corresponding author. E-mail: jfchen@sio.org.cn (Jianfang Chen)

Abstract

Paleo-climate proxy records documenting sea-ice extent are important sources of information to assess the time of emergence and magnitude of on-going changes in the Arctic Ocean and better predict future climate and environmental evolution in that region. In this study, a suite of geochemical tracers including total organic carbon (TOC), total nitrogen (TN), carbon/nitrogen ratio (C/N), stable isotope composition of organic carbon and nitrogen ($\delta^{13}C$, $\delta^{15}N$), and phytoplankton biomarkers (highly branched isoprenoids (HBIs) and sterols) were measured in a marine sediment core to document the sea-ice variability in the Chukchi Sea since the beginning of the Industrial Era. The downcore profile of the sea-ice proxy HBIs suggests a transition from extensive sea ice in the late 19th century to Marginal Ice Zone (MIZ) in AD 1930-1990s and then moderate sea-ice cover since 1990s. Rising of all HBI abundances between AD 1865-1875 indicate a transient retreat of summer ice edge off the shelf followed by a return to near-perennial sea ice till 1920-1930 as revealed by the absence of HBIs and brassicasterol. Sea ice retreat occurred again in AD 1920-1930 and followed by colder decades in 1940s-1960s before a sustained decline since the 1990s. The downcore profile of C/N, $\delta^{13}C$ of organic matter and sterols indicates a gradual increase of terrigenous inputs accelerating during the most recent decades likely due to enhanced fluvial run-off and sediment transport by sediment-laden sea ice. Concomitantly, increasing $\delta^{15}N$ values suggest limited nutrient utilization due to enhanced stratification of the surface ocean caused by increased freshening. The role of the Arctic Oscillation (AO), the Pacific Decadal Oscillation (PDO) and Atlantic Multidecadal Oscillation (AMO) are discussed to explore potential drivers of the observed sea-ice changes.

Key words: Sea ice, biomarkers, IP_{25}, HBI III, PIP_{25} index, Chukchi Sea

1. Introduction

Over the past decades, the Arctic Ocean has experienced dramatic climate and environmental changes including warming and rapid sea-ice retreat (Steele et al., 2008; Onarheim et al., 2018; Screen et al., 2018; Stroeve and Notz, 2018), increased inflow of Pacific Water (PW) (Woodgate, 2018; Woodgate and Peralta-Ferriz, 2021), enhanced freshening of surface waters (Yamamoto et al., 2009; Giles et al., 2012) and increased ocean acidification (Qi et al., 2017). These changes are having a strong impact on primary production (Arrigo et al., 2008; Arrigo and Van Dijken, 2015; Renaut et al., 2018) and marine ecosystems (Grebmeier, 2012; Wassmann et al., 2011), especially in the western Arctic Ocean where warming is more pronounced (Li et al., 2009; Coupel et al., 2012, 2015; Lee et al., 2019; Zhuang et al., 2020).

Sea ice is an essential component of Arctic climate and a key player in Arctic amplification (Thomas, 2017). The loss of sea ice affects heat and moisture exchanges between the ocean and the atmosphere and modifies deep-water formation through brine formation and ice melting (Petrich and Eicken, 2017) thereby altering the Arctic Ocean circulation (Aagaard and Carmack, 1989). Since the mid-20th century, thinning of sea ice combined with the lengthening of the melt season (Markus et al., 2009; Stroeve et al., 2014) and the loss of perennial multiyear ice have resulted in larger ice-free areas in summer (Holland et al., 2006), and in some regions, earlier melting (Wang and Overland, 2009, 2012). The western Arctic Ocean has undergone some of the most rapid and persistent decay of sea ice (Cavalieri and Parkinson, 2012; Serreze et al., 2016; Simmonds and Li., 2021). Climate projections predict a reduction of sea-ice cover duration of 20-36 days before 2050 in the southern Chukchi Sea, and up to 60 days in the East Siberian, Chukchi, and Beaufort Seas (Wang et al., 2018).

Sea-ice reconstructions provide a retrospective time frame to help decipher processes driving the long-term decline as well as decadal to centennial-scale variability of sea ice. Several biogenic and sedimentary proxies have been developed to obtain information on past sea ice conditions (Polyak et al., 2010; Kolling et al., 2020; Zhang and Xiao, 2021). Among them the molecular proxy, IP_{25} (Ice Proxy with 25 carbon atoms), a mono-unsaturated highly-branched isoprenoid (HBI) produced by few sea-ice diatoms has proven to be a valuable tool to assess seasonal sea ice cover from marine sediments (Belt et al., 2007; Sicre et al., 2013; Brown et al., 2014). Since the first reconstruction of Massé et al. (2008) in the North Atlantic, numerous studies have used

this biomarker in (sub)-polar oceanic regions (mostly of the northern hemisphere), often in combination with phytoplankton biomarkers (e.g., brassicasterol or dinosterol), in the so called 'PIP_{25} (Phytoplankton-IP_{25}) index' to produce semi-quantitatively seasonal sea-ice estimates (see reviews of Belt and Müller, 2013; Belt, 2018). More recently, a tri-unsaturated HBI (HBI III) has been proposed as an alternative to represent pelagic phytoplankton in order to improve the PIP_{25} index (Bai et al., 2019; Belt et al., 2015; Koch et al., 2020; Smik et al., 2016; Su et al., 2022) while Belt (2018) hypothesized that HBI II, also associated with sympagic algae, might provide an even better seasonal sea ice proxy than IP_{25}.

Historical data and high-resolution reconstructions of Arctic seasonal sea ice are still scarce (Kinnard et al., 2011; Walsh et al., 2016) and only a few paleo-records exist in the western Arctic Ocean (Pieńkowski et al., 2017; Stein et al., 2017; Astakhov et al., 2019, 2020; Kim et al., 2019; Koch et al., 2020). In the present study, we report on the downcore profiles of HBIs including IP_{25}, HBI II and HBI III as well of phytosterols, namely brassicasterol (24-methyl-5α-cholest-5,22E-dien-3β-ol) and dinosterol (4α, 23, 24-trimethyl-5α-cholest-22E-en-3β-ol) from a core retrieved in the northern Chukchi Sea. These biomarkers were analyzed to derive quantitative information on seasonal sea-ice evolution since AD 1850 and to explore causes of observed changes. Terrestrial biomarkers were also investigated as a complementary environmental information source of a changing Arctic Ocean.

2. Regional setting and material

The Chukchi Sea is one of the largest marginal seas in the world (Jakobsson, 2002). This region is strongly influenced by the northward PW inflow driven by salinity gradients between the Pacific and the Arctic Ocean (Coachman et al., 1975) (Fig. 1). In the Bering Strait, the PW splits into three main water masses i.e., the warmer, fresher and nutrient-depleted seasonal Alaska Coastal Water to the East (ACW; Hunt et al., 2013), the saline and nutrient-rich Anadyr Water (AW) to the West, and the Bering Shelf Water (BSW) in the central channel with moderate nutrient and salinity values (Weingartner et al., 2005). The surface hydrology of the region is also influenced by the Beaufort Gyre (BG) clockwise circulation driven by the Beaufort High winds (Proshutinsky and Johnson, 1997). In the past two decades, strong and more effective spin-up of the BG circulation has resulted in enhanced freshening in the western Arctic Ocean (Giles et al., 2012) with consequences on phytoplankton productivity and Arctic

ecosystem (Coupel et al., 2015; Ren et al., 2020). With the steepened decline of Arctic sea ice over the last four decades, the extent and thickness of sea ice in the Chukchi Sea has decreased more than any other marginal seas of the Arctic Ocean (Serreze and Stroeve, 2015; Onarheim et al., 2018). According to satellite observations, sea ice today is present from November to July and retreats during summer to reach a minimum over the northern Chukchi Sea in September (Fig. 1, https://nsidc.org, from Cavalieri et al., 1996).

The sediment core ARC4-C07 (72.54°N, 165.33°W, 51 m water depth) used in this study was retrieved from the shelf of the Chukchi Sea using a multi-corer during the 4th Chinese National Arctic Research Expedition (CHINARE) on board the R/V Xue Long in summer 2010 (Fig. 1; Table S1). The ARC4-C07 core (hereafter named C07) is located in an area where sea-ice cover is high in spring but close to the sea-ice edge in summer (Fig. 2). The 20-cm long sediment core was subsampled on board at 1 cm sampling interval from 0 to 10 cm and every 2 cm below 10 cm depth, and stored at 4°C until further treatment (See supplementary material for methods on the core chronology and biomarker analysis).

3. Results

3.1 Bulk parameter downcore profile

Fig. 3 shows the downcore profile of TOC (%), biogenic silica (%), TN (%), C/N molar ratio, $\delta^{13}C$ (‰) and $\delta^{15}N$ (‰) in the C07 core since AD 1850. TOC values range from 1.46 to 2.93% at the core top, with a mean value of 1.98%, and show a gradual increase towards present except for lower values from the late 1970s and early 1980s (Fig. 3a, Table S2). Biogenic silica shows broadly similar trends as TOC except for a sharp decay in the uppermost layer after a maximum of 17.3% at AD 1990 (Fig. 3b). TN content increases in a narrow range (0.15 to 0.34%) with lower values in the 1970s and at the end of the 19th century, similar to TOC. The C/N ratio show more variability between 7.8 and 11.5 with a mean value of 9.6. The $\delta^{13}C$ values of organic matter span from −22.3‰ to −23.6‰ at the core-top with a mean value of −22.7‰. The $\delta^{15}N$ values vary between 7.7‰ and 8.1‰ at the core-top with little changes downcore (Fig. 3c-f).

3.2 Biomarkers downcore profile

Generally, all biomarker concentrations show a broad increase towards present (Fig. 4, Table S2). IP_{25} is generally low until AD 1930, except for a brief increase around AD

1870 (1.4 μg/g TOC) coincident with decreasing TOC and biogenic silica values, followed by a gradual increase accelerating in the 1960s to reach highest values in the 1990s (4.2 μg/g TOC) (Fig. 4a). The downcore profile and range of concentrations of HBI II and IP_{25} are very similar, while HBI III is an order of magnitude lower, ranging from 0.01 to 0.47 μg/g TOC (Fig. 4b, c). Brassicasterol abundances are low until the abrupt increase in the 1990s to a maximum of 27.9 μg/g TOC (Fig. 4d). The dinosterol profile is quite different and shows strong decadal-scale variability that share resemblance with terrigenous biomarkers (campesterol and β-sitosterol) (Fig. 4e, f).

4. Discussion

4.1 Organic matter sources and trends

The high TOC content of the core top (2.93%) falls in the upper range of TOC values reported in surface sediments across the Chukchi Sea shelf (1.25~2.56%) by Goñi et al. (2013) (Table S2). TN values range from 0.15 to 0.34% (Table S2) and show significant positive correlation with TOC (r^2=0.68, $p<0.01$, Fig. 5) suggesting similar sources and fate of C and N. The C/N ratio has commonly been used to distinguish between algal and terrigenous organic matter (OM) (Hedges et al., 1986). Fresh marine algae typically exhibit C/N ratios around 4-6 whereas in vascular plants these values are above 20 (Meyers, 1994). C/N ratios $>$ 10 typically indicate significant terrestrial influence (Grebmeier et al., 1989). Downcore C/N values at C07 vary between 7.8 and 11.5 (mean value of 9.5, Table S2) indicating notable and increasing contribution of land-derived inputs since the late 1970s likely due to enhanced river run-off resulting thawing permafrost and ground ice melting induced by Arctic warming. The SCC flowing eastward towards the Chukchi shelf where it is diverted offshore by PW could occasionally contribute to the transport of terrestrial material to the core site (green arrows in Fig. 1). In addition, the central current BSW (blue arrow in Fig.1) is likely to carry fine sediment particles from the Bering Strait and shallow southern Chukchi shelf to C07 site (Weingartner et al., 2005; Darby et al., 2009; Yamamoto et al., 2017). A substantial amount of terrestrial organic matter to marine sediments may have be delivered via the melting of sea ice (Eicken et al., 2005). Lalande et al. (2007) also underlined commonly found high concentrations of lithogenic material in the lower layers of sea ice implying substantial contribution to vertical fluxes.

The $\delta^{13}C$ provides complementary information on organic carbon sources. Previous evaluation of isotopic end-members in the northern Bering and Chukchi Seas indicates distinctly $\delta^{13}C$ values for marine phytoplankton (-21.2‰) and terrigenous C_3 plant material (-27.0‰) (Naidu et al., 2000). However, it is important to note that the $\delta^{13}C$ values of OM from sea ice algae can vary between -15 to -18‰ (Schubert and Calvert, 2001). Belt et al. (2008) further reported that the mean $\delta^{13}C$ value for IP_{25} (-19.3‰) lies at the heavily ^{13}C-enriched marine end-member for Arctic OM. Therefore, $\delta^{13}C$ downcore values of -22.3‰ to -23.6‰ are likely indicative of marine sources with some contribution of isotopically lighter terrestrial organic material. More depleted $\delta^{13}C$ values towards present are also indicative of enhanced inputs from the land over the last decades as also inferred from C/N ratios (Fig. 3d) and higher amounts of campesterol and β-sitosterol, in particular since the 1960s (Fig. 4f).

The downcore profile of $\delta^{15}N$ values, spanning from 7.7 to 8.1‰, indicate a long-term increase. The $\delta^{15}N$ values of OM produced by plankton range between 7‰ and 10‰, whereas in C3 higher plants they are comprised between 0‰ and 2‰ (Meyers, 1997). The $\delta^{15}N$ trend may feature enhanced nutrient utilization by phytoplankton due limited nutrient availability under stratified conditions triggered by sea ice melting as postulated by Lee et al. (2012) based on N and C uptake rates. Increasing riverine freshwater inputs also contribute to ocean stratification and freshening of the Arctic Ocean (Li et al., 2009). A recent modeling study has shown that riverine water discharge would also impact significantly on the heat budget of the Arctic Ocean and consequently contribute to the sea-ice decline (Park et al., 2020).

4.2 Downcore profiles of biomarkers

As can be seen from Figure 4, sympagic HBIs (IP_{25} and HBI II) and pelagic biomarkers (HBI III, brassicasterol and dinosterol) display similar trends but at different concentration levels. The presence of IP_{25} and pelagic biomarkers throughout the core indicates seasonal sea-ice conditions at C07 since AD 1850 (Bai et al., 2019; Hu et al., 2020). All HBIs occur at extremely low levels in the older part of the record pointing out extensive sea-ice cover, except for a short interval of higher values between AD 1865 and AD 1875 (Fig. 4a-c). These results are consistent with historical sea ice data from whaling ship logbooks throughout the northern Bering Sea reporting more severe sea-ice conditions in the 1850s to 1860s, comparable to the 1970s taken as a reference for recent cold conditions (Mahoney et al., 2011). Indeed, while winter sea-

ice extent was similar during both periods, summer sea-ice extended further South in the Bering Strait in the 1850s to 1860s due to thicker sea ice and slower melting (Mahoney et al., 2011). The logbooks also describe a period of sea-ice retreat to the northern Bering Strait, which corresponds to sympagic HBIs and HBI III peaks found at AD 1865-1875 in our core (Mahoney et al., 2011; Fig. 4). Subsequent decades of the early 1900s are characterized by lower sympagic HBIs caused by a temporary return to colder conditions until a first stepwise increase at AD 1930 and second one in the 1990s (Fig. 4a-b). Stable HBI values in the 1940-60s are consistent with temporarily cold conditions reported by Mahoney et al. (2011).

The IP_{25} profile of the neighboring core ARA01B-03MUC (73.52°N, 168.94°W, 72.5m water depth; Fig. 1) located northwest of C07 shows similar features (Kim et al., 2019) (Fig. 6a). However, HBI III and brassicasterol decrease earlier in the upper ARA01B-03MUC, while IP_{25} declines synchronously in both cores. High brassicasterol together with high IP_{25} in ARA01B-03MUC since AD 1950 are indicative of sea-ice edge conditions. This is further supported by the co-eval lower and decreasing abundance of HBI III attesting the retreat of sea ice (0.15 to 0.07 µg g^{-1} TOC for ARA01B-03MUC versus 0.2 to 0.5 µg g^{-1} TOC for C07) (Fig. 6b).

The downcore profile of dinosterol is different from that of sympagic HBIs and brassicasterol (Fig. 4d-e). Low brassicasterol and HBI III from the late 19th century until AD 1920-1930 are coherent with extensive sea ice in the Chukchi Sea (Fig. 4). However, high amounts of dinosterol (i.e., >10 µg/g TOC) are surprising and could reflect other source organisms such as sea-ice microalgae as reported by Nichols et al. (1990) in sea ice samples from Antarctica. Note that the downcore profile of brassicasterol and dinosterol in ARA01B-03MUC show similar differences (Kim et al., 2019). Another common feature in C07 and ARA01B-03MUC is the recent decline of IP_{25} and brassicasterol, supporting accelerating summer sea ice retreat in the Chukchi Sea driven by climate change in recent decades (Fig. 6a, c).

Increased terrigenous sterols (campesterol and β-sitosterol) are consistent with C/N and $\delta^{13}C$ data and further evidence high and increasing river run-off (Fig. 4f). With the decline of sea ice, airborne continentally-derived material from adjacent continents could also contribute more to Arctic sediments. Indeed, in addition to fluvial deposits, terrestrial constituents transported over long distances from their emission sources as aerosols accumulate in sea ice and get released during the melting season. This is

evidenced by terrigenous *n*-alkanes at station DM (Fig. 1) showing high export fluxes as sea ice breaks-up in summer (Bai et al, 2019). Ren et al. (2020) also reported similar results with high terrigenous campesterol and β-sitosterol fluxes in summer contrasting with no detectable export in winter.

4.3 HBIs and phytosterols as proxies of seasonal sea ice

Semi-quantitative estimates of sea ice can be calculated from the PIP_{25} index by combining sympagic IP_{25} with pelagic phytoplankton biomarkers using the following expression:

$$PIP_{25} = \frac{[IP_{25}]}{[IP_{25}] + [phytoplankton\ biomarker] * c}$$

$$\text{with } c = \frac{mean\ IP_{25}\ concentration}{mean\ phytoplankton\ biomarker\ concentration}$$

where c is a balance factor accounting for the different magnitude concentrations between IP_{25} and phytoplankton biomarkers, such as brassicasterol and dinosterol that were used as the phytoplankton end-member to derive P_BIP_{25}, P_DIP_{25}. More recently, HBI III has also been proposed as an alternative pelagic phytoplankton end-member to calculate $P_{III}IP_{25}$ index.

Indeed, surface sediments from the Barents and Chukchi seas have shown elevated abundances of HBI III in the vicinity of the sea-ice edge or in the MIZ (Belt et al., 2015; Smik et al., 2016; Ribeiro et al., 2017; Belt, 2018; Bai et al., 2019). Yet, different relationships of this compound to sea ice have been postulated. For example, maximum HBI III in surface sediments from the western Barents Sea has been associated with winter sea-ice extent and/or the MIZ (Belt et al., 2015) while Ribeiro et al. (2017) correlated HBI III in East Greenland fjord sediments to mid-July MIZ conditions. Uncertainties still remain as to the HBI III producers and habitat mainly because of the lack of modern ocean observations. Knowledge on HBI III has been essentially inferred from correlations between concentrations in surface sediments and SIC at different seasons. The only sediment trap data on HBI III in the Arctic Ocean are from Bai et al. (2019) at station DM (Fig. 1) that shows high fluxes at moderate sea-ice cover (< 50%) and their decrease towards ice-free conditions that are consistent with production by sea-ice edge thriving diatoms. Furthermore, cross-plots of HBI III against IP_{25} downcore concentrations exhibit a stronger positive relationship than brassicasterol against IP_{25} (Fig. S2) in agreement with HBI III production being closely associated

with the sea-ice edge. This interpretation is also supported by co-eval higher fluxes of the IP_{25} and HBI III from end of July to early August at the station DM (Bai et al., 2019). Synchronous changes of IP_{25} and HBI III have been further interpreted by Belt (2018) as reflecting rapidly changing sea ice (advancing and retreating) such as for example the two-step concomitant rise of HBI III and IP_{25} in the1970s and early 1990s in our core (Fig. 6a, b; Fig. 7; Smik et al., 2016; Belt, 2018; Bai et al., 2019).

HBI III, as well as brassicasterol and dinosterol were thus used to calculate PIP_{25} indexes and derive semi-quantitively sea ice changes since AD 1850. On average, concentrations of brassicasterol were about five times higher, dinosterol about twelvefold higher and HBI III about twelve times lower than IP_{25}, resulting in balance factor *c* of 0.20, 0.08 and 11.74, respectively. Downcore P_BIP_{25} values vary between 0.19 and 0.79, which according to Müller et al. (2011), correspond to low sea ice to MIZ conditions, with only one value above the permanent sea-ice cover threshold (i.e. P_BIP_{25} >0.75) (Fig. 6d). The sharp drop in the 1920s -1930s suggests a transient period of sea-ice retreat (Fig. 7a). Since AD 1930, P_BIP_{25} values increase from 0.54 to 0.74, indicating proximal MIZ conditions except for the last decade of accelerated decline (Fig. 6d, Table S2). Indeed, P_BIP_{25} shows a decreasing trend towards less/variable sea-ice cover since the late 1990s as expected from the recent unprecedented decline of sea ice in the northern Chukchi Sea (Walsh et al., 2016). $P_{III}IP_{25}$ values show different trends and variability that share more resemblance with the sea ice extent in the Chukchi Sea of Walsh et al. (2016) with relatively high and stable values from the 1880s to the 1920s followed by a continuing decrease reflecting the progressive and long-term retreat of seasonal sea ice extent (Fig. 6d, Table S2). Yet, the drastic reduction of the last decades is not reproduced by the $P_{III}IP_{25}$ index. This result can be explained by HBI III production tending to zero as surface waters become ice-free during summer as opposed to brassicasterol (Bai et al., 2019). The P_DIP_{25} values show similar features as P_BIP_{25}, despite discrepancies between dinosterol and brassicasterol profiles, except since the 1980s when P_DIP_{25} indicates increased sea ice contrary to observations (Walsh et al., 2016) (Fig. 4d, e and 6d). Diverging spatial distribution of these two sterols has also been underlined by Su et al. (2022) in the Eastern Siberian Sea. It has been speculated that dinosterol in the Arctic Ocean might be produced by other organisms than dinoflagellates (Nichols et al., 1990). Due to remaining source uncertainties of this sterol in the Arctic Ocean and inconsistent trends at moderate to low sea ice, P_DIP_{25}, was not further considered for sea-ice reconstruction.

Finally, the tri-unsaturated HBI ratio (HBI TR_{25}) was also calculated using the following equation of Belt et al. (2019) (HBI TR_{25}= [Z-triene]/ ([Z-triene] + [E-triene])) to explore this new biomarker as a potential proxy of spring phytoplankton bloom in the Arctic and sub-Arctic. The downcore values of HBI TR_{25} are all below the spring phytoplankton bloom threshold of 0.62 from which we can conclude that primary production did not reach high levels as suggested by the $\delta^{15}N$ values pointing out limited nutrient availability of surface waters (Fig. 6e).

4.4. Centennial-scale variability of sea-ice and potential key physical drivers

SIC reconstruction. In order to translate the downcore profiles of $P_{III}IP_{25}$ and P_BIP_{25} into SIC, we performed sensitivity tests using the surface sediment dataset from the Chukchi Sea of Bai et al. (2019) and the monthly SIC values from satellite data for June, July, August and September as well as for the summer months (July-September, JAS); SuSIC) (Fig. S4 and S5). $P_{III}IP_{25}$ in surface sediments shows a stronger correlation with SuSIC (r^2=0.47, p<0.01) than P_BIP_{25} r^2=0.09, p<0.01) (Fig. S3; Bai et al., 2019). Furthermore, downcore P_BIP_{25} derived SuSIC yield negative values at low sea ice and values exceeding 100% at high sea ice (Fig. S6). The SuSIC obtained from $P_{III}IP_{25}$ leads to generally lower estimates and negative values over the most recent decades. Reconstructions obtained from $P_{III}IP_{25}$ and P_BIP_{25} for June, July, August and September (Fig. S4 and S5) show similar trends as for SuSIC but differ in absolute values (Fig. S6). As found for SuSIC, correlations between monthly SIC and $P_{III}IP_{25}$ were stronger than with P_BIP_{25}. June seems to provide the best downcore SIC estimates and range of variation, and $P_{III}IP_{25}$ to perform better than P_BIP_{25} (Fig. S6). Yet the steep decline of the last decades (Fig. 7g) is not reproduced by our reconstruction possibly because of smoothing effect due to the temporal resolution (on average of 10 years) or low HBI III production as highlighted earlier. In contrast, P_BIP_{25} still overestimate SIC at high sea ice and underestimate SIC at low SIC (Fig. S6).

Key physical drivers. Important parameters affecting Arctic sea ice include winds and ice motion, cloud cover, ice albedo feedback and ocean heat advection (Perovich, 2011). Modes of climate variability such as the Arctic Oscillation (AO, Thompson and Wallace, 1998), the Pacific Decadal Oscillation (PDO, Mantua et al.,1997), and the Atlantic Multidecadal Oscillation (AMO, Enfield, 2001) can have an impact on sea ice variability on decadal time scales (Frey et al., 2015; Mahajan et al., 2011). In order to

evaluate the role of these factors in the northern Chukchi Sea, our data were compared to AO, PDO, and AMO indices as well as to the Arctic surface air temperature (Fig. 7).

Links with the AO. The AO is a major atmospheric circulation feature of the mid- to high latitudes of the Northern Hemisphere. Several studies have recognized the complex relationship between Arctic sea ice and AO or its expression in the North Atlantic, the North Atlantic Oscillation (NAO) (Rigor et al., 2002; Danielson et al., 2011; Stroeve et al., 2011; Yang et al., 2016; Luo et al., 2017). In the Arctic, the AO is known to affect sea ice motion through surface winds thereby altering sea ice thickness and concentration. A positive and significant correlation was demonstrated between summer AO and sea ice in the Chukchi Sea (see Fig. 13d from Frey et al. 2015). Indeed, during summer season, negative AO promotes southeasterly winds bringing warm air over the Chukchi Sea decreasing the sea ice cover, a mechanism that could account for the long-term AO weakening and associated sea-ice decline from AD 1920-1930s to the 1970s (Fig. 7f, g). On the other hand, during positive AO the transport and piling up of old sea ice pushed by northeasterly winds result in extensive summer sea ice in the Chukchi and Beaufort seas such as found in the late 1800s – early 1900s (Frey et al., 2015). However, in the recent decade of positive AO, warmer surface ocean would have favored sea ice melting preventing its accumulation (Wang et al, 2009; Stroeve et al., 2011), leading instead to sea ice decline at unprecedented rate as illustrated by the ice-free period reconstruction from the nearby 14R07 of Astakhov et al. (2019) (Fig. 7e).

Links with the PDO. The PDO is another factor of sea-ice variability at decadal timescales. The PDO is defined as the leading empirical orthogonal function of monthly sea surface temperature in the North Pacific, North of 20°N (Mantua et al., 1997). Instrumental data show that the PDO was predominantly positive for the 1922-1944 period, negative between 1945 and 1976, and positive again between 1977 and 1990 (Rodionov et al., 2007; Wendler et al., 2014; Fig. 7c). Negative PDO in the early 20th century (AD 1910-1920) corresponds to high sea-ice cover while the subsequent positive PDO years (AD 1922-1944) are associated with decreasing sea ice in our record. These results are in accordance with the negative correlation between summer PDO and sea ice in the Chukchi Sea although not statistically significant (see Fig.13c in Frey et al., 2015). However, negative PDO years since 1940 seem to roughly coincide with decreasing sea ice suggesting that this relationship would not hold since the mid-20th century. Furthermore, negative PDO phases coincide with colder years in the

Arctic air temperature record except for the last warmer decades possibly reflecting overprinting of the global warming trend as suggested for AO (Fig. 7b, Connolly et al., 2017).

Links with the AMO and AMOC. The AMO, which is thought to be mainly driven by the Atlantic Meridional Overturning Circulation (AMOC), has been investigated as an additional possible source of natural variability of sea ice. In fact, the AMO also has been found to have an impact on Eurasian surface air temperature (Luo et al., 2017). Control simulations using the GFDL CM2.1 model have shown a strong negative correlation between both AMO and AMOC and Arctic sea ice at all seasons (Mahajan et al., 2011). Comparison of AMO with our data broadly shows opposite sign evolution with extensive sea ice until 1910s-1920s at negative AMO, followed by decreasing sea ice until the 1960s as AMO increases (Fig. 7d, e). Thereafter, this relationship seems to attenuate. According to Mahajan et al. (2011), the influence of AMO on the recent summer sea ice decline would have been weak compared to the response of sea ice to AO. This finding is further supported by CMIP3 coupled general circulation model simulations using pre-industrial forcing of Day et al. (2012) showing that the AMO shift from negative to positive phase between 1979 and 2010 accounted for only 0.5–3.1%/decade of the 10.1%/decade of September sea ice decline. If confirmed, this result would suggest that the North Atlantic heat transported to the Arctic would not be as determinant in sea ice changes in the Chukchi Sea. Very recently Luo et al. (2022) further highlighted the joint effect of AMO and PDO on the decadal variability of Arctic air temperatures. The loss of summer Arctic sea ice and flushing of multi-layer sea ice out of basin in the past decade has already changed the atmospheric circulation. The overprinting effect of global warming in the Arctic may have caused different environmental mechanisms and feedbacks that could explain changes in the relationship between sea ice, air temperature and climatic drivers.

5. Conclusions

The downcore record of sea ice proxies since AD 1850 allowed to improve semi-quantitative assessment of sea ice and gain insights into past sea ice and environmental changes in the Chukchi Sea. Bulk parameters and sterol data along the core indicate increase terrestrial material to the sediments due to enhanced continental run-off, sediment transport by sediment-laden sea ice and airborne inputs. The $\delta^{15}N$ data indicate gradual nutrient limitation of phytoplankton growth due to enhance

stratification induced by surface freshening.

Among PIP_{25} indexes, $P_{III}IP_{25}$ appears to best reproduce trends and variability of sea ice in the Chukchi Sea. Our data also question the use of dinosterol as an end-member for pelagic phytoplankton in the Arctic Ocean due to potential bias of sea ice microalgae producing dinosterol that would deserve further investigation on sea ice samples. The sea ice reconstruction based on $P_{III}IP_{25}$ shows variations that are coherent with the positive and statistically significant relationship with the summer AO evidenced by Frey et al. (2015). Notably, the sea-ice retreat in the 1865s-1875s and from the 1920s to the 1970-1980s are co-eval with negative AO phases, while extensive sea-ice cover in the 1910-1920s occurs during positive AO. However, this negative relationship between AO and seasonal sea ice seems to have been altered by global warming overprinting effect over the last decades. Our results also suggest a minor role of PDO and AMO on seasonal sea ice as compared to AO since the 20th century in agreement with model experiments.

Acknowledgements

We are grateful to the captain, crew members and scientific party of the R/V *Xuelong* for their help with the retrieve of the sediment core. We are grateful to Fanny Kaczmar who helped produce HBI data at the LOCEAN, Sorbonne Université, Campus Pierre et Marie Curie (Paris), and to Dr. Guillaume Massé for supplying the chemical standards. This study was funded by the Scientific Research Funds of the Second Institute of Oceanography, State Oceanic Administration, China (No. JG1911), the National Natural Science Foundation of China (Nos. 41976229, 41306200, 41606052, 41941013), the National Key Research and Development Program of China (Nos. 2019YFC1509101, 2019YEE0120900), the Chinese Polar Environmental Comprehensive Investigation and Assessment Programs (No. CHINARE 0304), and the project ICAR (Sea Ice melt, Carbon, Acidification and Phytoplankton in the present and past Arctic Ocean) funded by Cai Yuan Pei Program. We also thank the Centre National de la Recherche Scientifique (CNRS) for M.-A.S. salary. We are grateful to the two anonymous reviewers who provided constructive suggestions for the manuscript improvement.

Data availability statement

All data that support the findings of this study are included within the article (and supplementary information files).

Author contributions

Y.B. designed the study and wrote the manuscript with contribution of M.-A.S., J.R., B.J., J.C., H.L. and H.J. V.K. and Z.J. contributed the biomarker analyses. L.L. retrieved the environmental data from different database. Q.Z. contributed the biogenic silica and L.S. performed the determination of TOC. All authors contributed to the final version of the manuscript.

Declarations of interest: None

References

Aagaard, K., Carmack, E.C., 1989. The role of sea ice and other fresh water in the Arctic circulation. Journal of Geophysical Research: Oceans 94, 14485-14498.

Arrigo, K.R., van Dijken, G., Pabi, S., 2008. Impact of a shrinking Arctic ice cover on marine primary production. Geophysical Research Letters 35, L19603, doi: 10.1029/2008GL035028.

Arrigo, K.R., van Dijken, G.L., 2015. Continued increases in Arctic Ocean primary production. Progress in Oceanography 136, 60-70.

Astakhov, A.S., Bosin, A.A., Liu, Y.G., Darin, A.V., Kalugin, I.A., Artemova, A.V., Babich, V.V., Melgunov, M.S., Vasilenko, Y.P., Vologina, E.G., 2019. Reconstruction of ice conditions in the northern Chukchi Sea during recent centuries: Geochemical proxy compared with observed data. Quaternary International 522, 23-37.

Astakhov, A.S., Shi, X., Darin, A.V., Kalugin, I.A., Hu, L., Tsoy, I.B., Kolesnik, A.N., Obrezkova, M.S., Alatortsev, A.V., Babich, V.V., Plotnikov, V.V., 2020. Reconstructing ice conditions in the southern Chukchi Sea during the last millennium based on chemical composition of sediments and diatom assemblages. Marine Geology 427, 106220.

Bai, Y., Sicre, M.-A., Chen, J., Klein, V., Jin, H., Ren, J., Li, H., Xue, B., Ji, Z., Zhuang, Y., Zhao, M., 2019. Seasonal and spatial variability of sea ice and phytoplankton biomarker flux in the Chukchi Sea (western Arctic Ocean). Progress in Oceanography 171, 22-37.

Belt, S.T., 2018. Source-specific biomarkers as proxies for Arctic and Antarctic sea ice. Organic Geochemistry 125, 277-298.

Belt, S.T., Cabedo-Sanz, P., Smik, L., Navarro-Rodriguez, A., Berben, S.M.P., Knies, J., Husum, K., 2015. Identification of paleo Arctic winter sea ice limits and the marginal ice zone: Optimised biomarker-based reconstructions of late Quaternary

Arctic sea ice. Earth and Planetary Science Letters 431, 127-139.

Belt, S.T., Massé, G., Rowland, S.J., Poulin, M., Michel, C., LeBlanc, B., 2007. A novel chemical fossil of palaeo sea ice: IP_{25}. Organic Geochemistry 38, 16-27.

Belt, S.T., Massé, G., Vare, L.L., Rowland, S.J., Poulin, M., Sicre, M.-A., Sampei, M., Fortier, L., 2008. Distinctive 13C isotopic signature distinguishes a novel sea ice biomarker in Arctic sediments and sediment traps. Marine Chemistry 112, 158-167.

Belt, S.T., Müller, J., 2013. The Arctic sea ice biomarker IP_{25}: a review of current understanding, recommendations for future research and applications in palaeo sea ice reconstructions. Quaternary Science Reviews 79, 9-25.

Belt, S.T., Smik, L., Köseoğlu, D., Knies, J., Husum, K., 2019. A novel biomarker-based proxy for the spring phytoplankton bloom in Arctic and sub-arctic settings – HBI T25. Earth and Planetary Science Letters 523, 115703.

Brown, T.A., Belt, S.T., Tatarek, A., Mundy, C.J., 2014. Source identification of the Arctic sea ice proxy IP_{25}. Nature communications 5, 4197.

Caesar, L., Rahmstorf, S., Robinson, A., Feulner, G., Saba, V., 2018. Observed fingerprint of a weakening Atlantic Ocean overturning circulation. Nature 556, 191–196.

Cavalieri, D.J., Parkinson, C.L., 2012. Arctic sea ice variability and trends, 1979–2010. Cryosphere 6 (4), 881–889. http://dx.doi.org/10.5194/tc-6-881-2012.

Cavalieri, D.J., Parkinson, C.L., Gloersen, P., Zwally, H.J., 1996, updated yearly. Sea Ice Concentrations from Nimbus-7 SMMR and DMSP SSM/I-SSMIS Passive Microwave Data, Version 1. [Indicate subset used]. Boulder, Colorado USA. NASA National Snow and Ice Data Center Distributed Active Archive Center. doi: https://doi.org/10.5067/8GQ8LZQVL0VL.

Coachman, L.K., Aagaard, K., Tripp, R.B., 1975. Bering Strait: the regional physical

oceanography. University of Washington Press: Seattle, WA (172pp).

Connolly, R., Connolly, M., Soon, W., 2017. Re-calibration of Arctic sea ice extent datasets using Arctic surface air temperature records. Hydrological Sciences Journal 62, 1317-1340.

Coupel, P., Jin, H., Joo, M., Horner, R., Bouvet, H.A., Sicre, M., Gascard, J., Chen, J., Garcon, V., Ruizpino, D., 2012. Phytoplankton distribution in unusually low sea ice cover over the Pacific Arctic. Biogeosciences 9, 4835-4850.

Coupel, P., Ruiz-Pino, D., Sicre, M.-A., Chen, J., Lee, S., Schiffrine, N., Li, H., Gascard, J.-C., 2015. The impact of freshening on phytoplankton production in the Pacific Arctic Ocean. Progress in Oceanography 131, 113-125.

Danielson, S., Curchitser, E., Hedstrom, K., Weingartner, T., Stabeno, P., 2011. On ocean and sea ice modes of variability in the Bering Sea. Journal of Geophysical Research. Oceans 116, C12034. https://doi.org/10.1029/2011JC007389.

Darby, D.A., Ortiz, J., Polyak, L., Lund, S., Woodgate, R.A., 2009. The role of currents and sea ice in both slowly deposited central Arctic and rapidly deposited Chukchi-Alaskan margin sediments. Global and Planetary Change 68, 58-72.

Day, J.J., Hargreaves, J.C., Annan, J.D., Abe-Ouchi, A., 2012. Sources of multi-decadal variability in Arctic sea ice extent. Environmental Research Letters 7, 034011.

Eicken, H., Gradinger, R., Gaylord, A., Mahoney, A., Rigor, I., Melling, H., 2005. Sediment transport by sea ice in the Chukchi and Beaufort Seas: Increasing importance due to changing ice conditions? Deep-Sea Research Part II 52, 3281-3302.

Enfield, D.B., Mestas-Nuñez, A.M., Trimble, P.J., 2001. The Atlantic Multidecadal Oscillation and its relation to rainfall and river flows in the continental U.S. Geophysical Research Letters 28, 2077-2080.

Frey, K.E., Moore, G.W.K., Cooper, L.W., Grebmeier, J.M., 2015. Divergent patterns of recent sea ice cover across the Bering, Chukchi, and Beaufort seas of the Pacific Arctic Region. Progress in Oceanography 136, 32-49.

Giles, K.A., Laxon, S.W., Ridout, A.L., Wingham, D.J., Bacon, S., 2012. Western Arctic Ocean freshwater storage increased by wind-driven spin-up of the Beaufort Gyre. Nature Geoscience 5, 194-197.

Goñi, M.A., O'Connor, A.E., Kuzyk, Z.Z., Yunker, M.B., Gobeil, C., Macdonald, R.W., 2013. Distribution and sources of organic matter in surface marine sediments across the North American Arctic margin. Journal of Geophysical Research: Oceans 118, 4017-4035.

Grebmeier, J., Feder, H., Mcroy, C., 1989. Pelagic benthic coupling on the shelf of the northern Bering and Chukchi Seas-II. Benthic community structure. Marine Ecology Progress Series 51, 253-268.

Grebmeier, J.M., 2012. Shifting patterns of life in the Pacific Arctic and Sub-arctic Seas. Annual Review of Marine Science, 4, 63–78.

Halfar, J., Williams, B., Hetzinger, S., Steneck, R.S., Lebednik, P., Winsborough, C., Omar, A., Chan, P., Wanamaker, A.D., Jr., 2011. 225 years of Bering Sea climate and ecosystem dynamics revealed by coralline algal growth-increment widths. Geology 39, 579-582.

Hedges, J.I., Clark, W.A., Quay, P.D., Richey, J.E., Devol, A.H., Santos, M., 1986. Compositions and fluxes of particulate organic material in the Amazon River. Limnology and Oceanography 31, 717-738.

Holland, M.M., Bitz, C.M., Tremblay, B., 2006. Future abrupt reductions in the summer Arctic sea ice. Geophysical Research Letters 33, L23503. http://dx.doi.org/10.1029/2006GL028024.

Hu, L., Liu, Y., Xiao, X., Gong, X., Zou, J., Bai, Y., Gorbarenko, S., Fahl, K., Stein,

R., Shi, X., 2020. Sedimentary records of bulk organic matter and lipid biomarkers in the Bering Sea: A centennial perspective of sea-ice variability and phytoplankton community. Marine Geology 429, 106308.

Hunt, J.G.L., Blanchard, A.L., Boveng, P., Dalpadado, P., Drinkwater, K.F., Eisner, L., Hopcroft, R.R., Kovacs, K.M., Norcross, B.L., Renaud, P., 2013. The Barents and Chukchi Seas: Comparison of two Arctic shelf ecosystems. Journal of Marine Systems 109–110, 43-68.

Jakobsson, M., 2002. Hypsometry and volume of the Arctic Ocean and its constituent seas. Geochemistry Geophysics Geosystems 3, 1-18.

Kim, J.-H., Gal, J.-K., Jun, S.-Y., Smik, L., Kim, D., Belt, S.T., Park, K., Shin, K.-H., Nam, S.-I., 2019. Reconstructing spring sea ice concentration in the Chukchi Sea over recent centuries: insights into the application of the PIP_{25} index. Environmental Research Letters 14, 125004.

Kinnard, C., Zdanowicz, C.M., Fisher, D.A., Isaksson, E., de Vernal, A., Thompson, L.G., 2011. Reconstructed changes in Arctic sea ice over the past 1,450 years. Nature 479, 509-512.

Koch, C.W., Cooper, L.W., Lalande, C., Brown, T.A., Frey, K.E., Grebmeier, J.M., 2020. Seasonal and latitudinal variations in sea ice algae deposition in the Northern Bering and Chukchi Seas determined by algal biomarkers. PLOS ONE 15, e0231178. https://doi.org/10.1371/journal.pone.0231178.

Kolling, H.M., Stein, R., Fahl, K., Sadatzki, H., de Vernal, A., Xiao, X., 2020. Biomarker distributions in (sub)-Arctic surface sediments and their potential for sea-ice reconstructions. Geochemistry, Geophysics, Geosystems 21, e2019GC008629. https://doi.org/10.1029/2019GC008629.

Lalande, C., Grebmeier, J.M., Wassmann, P., Cooper, L.W., Flint, M.V., Sergeeva, V.M., 2007. Export fluxes of biogenic matter in the presence and absence of

seasonal sea ice cover in the Chukchi Sea. Continental Shelf Research 27, 2051-2065.

Lee, S.H., Joo, H.M., Liu, Z., Chen, J., He, J., 2012. Phytoplankton productivity in newly opened waters of the Western Arctic Ocean. Deep Sea Research Part II: Topical Studies in Oceanography 81-84, 18-27.

Lee, Y., Min, J.-O., Yang, E.J., Cho, K.-H., Jung, J., Park, J., Moon, J.K., Kang, S.-H., 2019. Influence of sea ice concentration on phytoplankton community structure in the Chukchi and East Siberian Seas, Pacific Arctic Ocean. Deep-Sea Research Part I, 147, 54-64, doi: https://doi.org/10.1016/j.dsr.2019.04.001.

Li, J., and Wang, J. X. L., 2003. A modified zonal index and its physical sense. Geophysical Research Letters 30, 1632, doi: 10.1029/2003GL017441, 12.

Li, W.K., Mclaughlin, F.A., Lovejoy, C., Carmack, E.C., 2009. Smallest algae thrive as the Arctic Ocean freshens. Science 326, 539.

Luo, B., Luo, D., Wu, L., Zhong, L., Simmonds, I., 2017. Atmospheric circulation patterns which promote winter Arctic sea ice decline. Environmental Research Letters 12, 054017.

Luo, B., Luo, D., Dai, A., Simmonds, I., Wu, L., 2022. Decadal Variability of Winter Warm Arctic-Cold Eurasia Dipole Patterns Modulated by Pacific Decadal Oscillation and Atlantic Multidecadal Oscillation. Earth's Future 10, e2021EF002351.

Luo, D., Chen, Y., Dai, A., Mu, M., Zhang, R., Ian, S., 2017. Winter Eurasian cooling linked with the Atlantic Multidecadal Oscillation. Environmental Research Letters 12, 125002.

Mahajan S, Zhang, R. and Delworth, T.L., 2011. Impact of the Atlantic Meridional Overturning Circulation (AMOC) on Arctic Surface Air Temperature and Sea Ice Variability. Journal of Climate 24, 6573–6581.

Mahoney, A. R., Bockstoce, J., Botkin, D. B., Eicken, H., Nisbet, R. A., 2011. Sea-Ice Distribution in the Bering and Chukchi Seas: Information from Historical Whaleships' Logbooks and Journals. Arctic 64, 465-477.

Mantua, N.J., Hare, S.R., Zhang, Y., Wallace, J.M., Francis, R.C., 1997. A Pacific interdecadal climate oscillation with impacts on salmon production. Bulletin of the American Meteorological Society 78, 1069-1080.

Markus, T., Stroeve, J.C., Miller, J., 2009. Recent changes in Arctic sea ice melt onset, freezeup, and melt season length. Journal of Geophysical Research-Oceans 114. http://dx.doi.org/10.1029/2009jc005436.

Massé, G., Rowland, S.J., Sicre, M.-A., Jacob, J., Jansen, E., Belt, S.T., 2008. Abrupt climate changes for Iceland during the last millennium: Evidence from high resolution sea ice reconstructions. Earth and Planetary Science Letters 269, 565-569.

Meyers, P.A., 1994. Preservation of elemental and isotopic source identification of sedimentary organic matter. Chemical Geology 114, 289-302.

Meyers, P.A., 1997. Organic geochemical proxies of paleoceanographic, paleolimnologic, and paleoclimatic processes. Organic Geochemistry 27, 213-250.

Müller, J., Wagner, A., Fahl, K., Stein, R., Prange, M., Lohmann, G., 2011. Towards quantitative sea ice reconstructions in the northern North Atlantic: A combined biomarker and numerical modelling approach. Earth and Planetary Science Letters 306, 137-148.

Naidu, A.S., Cooper, L.W., Finney, B.P., Macdonald, R.W., Alexander, C., Semiletov, I.P., 2000. Organic carbon isotope ratios (δ13C) of Arctic Amerasian Continental shelf sediments. International Journal of Earth Sciences 89, 522-532.

Nichols, P.B., Palmisano, A.C., Rayner, M.S., Smith, G.A., White, D.C., 1990.

Occurrence of novel C30 sterols in Antarctic Sea-ice diatoms communities during the spring bloom. Organic Geochemistry 15, 503-508.

Onarheim, I.H., Eldevik, T., Smedsrud, L.H., Stroeve, J.C., 2018. Seasonal and Regional Manifestation of Arctic Sea Ice Loss. Journal of Climate 31, 4917-4932.

Park, H., Watanabe, E., Kim, Y., Polyakov, I., Oshima, K., Zhang, X., Kimball, J.S., Yang, D., 2020. Increasing riverine heat influx triggers Arctic sea ice decline and oceanic and atmospheric warming. Science Advance 6, EABC4699.

Perovich, D.K., 2011. The changing arctic sea ice cover. Oceanography 24, 162–173.

Petrich, C., Eicken, H., 2017. Overview of sea ice growth and properties. In: Thomas, D.N.(Ed.), Sea Ice, 3rd ed. John Wiley & Sons, Chichester, pp. 1–41.

Pieńkowski, A.J., Gill, N.K., Furze, M.F., Mugo, S.M., Marret, F., Perreaux, A., 2017. Arctic sea-ice proxies: Comparisons between biogeochemical and micropalaeontological reconstructions in a sediment archive from Arctic Canada. The Holocene 27, 665-682.

Polyak, L., Alley, R.B., Andrews, J.T., Brigham-Grette, J., Cronin, T.M., Darby, D.A., Dyke, A.S., Fitzpatrick, J.J., Funder, S., Holland, M., Jennings, A.E., Miller, G.H., O'Regan, M., Savelle, J., Serreze, M., St. John, K., White, J.W.C., Wolff, E., 2010. History of sea ice in the Arctic. Quaternary Science Reviews 29, 1757-1778.

Polyakov, I.V., Alekseev, G.V., Bekryaev, R.V., Bhatt, U., Colony, R.L., Johnson, M.A., Karklin, V.P., Makshtas, A.P., Walsh, D., Yulin, A.V., 2002. Observationally based assessment of polar amplification of global warming. Geophysical Research Letters 29, 1878, doi: 10.1029/2001GL011111.

Proshutinsky, A.Y., Johnson, M.A., 1997. Two circulation regimes of the wind-driven Arctic Ocean. Journal of Geophysical Research: Oceans 102, 12493-12514.

Qi, D., Chen, L., Chen, B., Gao, Z., Zhong, W., Feely, Richard A., Anderson, Leif G.,

Sun, H., Chen, J., Chen, M., Zhan, L., Zhang, Y., Cai, W.-J., 2017. Increase in acidifying water in the western Arctic Ocean. Nature Climate Change 7, 195-199.

Ren, J., Chen, J., Bai, Y., Sicre, M.-A., Yao, Z., Lin, L., Zhang, J., Li, H., Wu, B., Jin, H., Ji, Z., Zhuang, Y., Li, Y., 2020. Diatom composition and fluxes over the Northwind Ridge, western Arctic Ocean: impact of marine surface circulation and sea ice distribution. Progress in Oceanography, 186, 102377. https://doi.org/10.1016/j.pocean.2020.102377.

Renaut, S., Devred, E., Babin, M., 2018. Northward Expansion and Intensification of Phytoplankton Growth during the Early Ice-Free Season in Arctic. Geophysical Research Letters 45, 10,590-10,598.

Ribeiro, S., Sejr, M.K., Limoges, A., Heikkilä, M., Andersen, T.J., Tallberg, P., Weckström, K., Husum, K., Forwick, M., Dalsgaard, T., Massé, G., Seidenkrantz, M.-S., Rysgaard, S., 2017. Sea ice and primary production proxies in surface sediments from a High Arctic Greenland fjord: Spatial distribution and implications for palaeoenvironmental studies. Ambio 46, 106-118.

Rigor, I.G., Wallace, J.M., Colony, R.L., 2002. Response of Sea Ice to the Arctic Oscillation. Journal of Climate 15, 2648-2663.

Rodionov, S.N., Bond, N.A., Overland, J.E., 2007. The Aleutian Low, storm tracks, and winter climate variability in the Bering Sea. Deep Sea Research Part II: Topical Studies in Oceanography 54, 2560-2577.

Schubert, C.J., Calvert, S.E., 2001. Nitrogen and carbon isotopic composition of marine and terrestrial organic matter in Arctic Ocean sediments: implications for nutrient utilization and organic matter composition. Deep Sea Research Part I: Oceanographic Research Papers 48, 789-810.

Screen, J.A., Bracegirdle, T.J., Simmonds, I., 2018. Polar Climate Change as Manifest in Atmospheric Circulation. Current Climate Change Reports 4, 383–395.

Serreze, M. C., & Stroeve, J., 2015. Arctic sea ice trends, variability and implications for seasonal ice forecasting. Philosophical transactions. Series A, Mathematical, physical, and engineering sciences 373(2045), 20140159. https://doi.org/10.1098/rsta.2014.0159.

Serreze, M.C., Crawford, A.D., Stroeve, J.C., Barrett, A.P., Woodgate, R.A., 2016.Variability, trends, and predictability of seasonal sea ice retreat and advance in the Chukchi Sea. Journal of Geophysical Research: Oceans 121. https://doi.org/10.1002/2016JC011977.

Sicre, M.-A., Khodri, M., Mignot, J., Eiríksson, J., Knudsen, K.-L., Ezat, U., Closset, I., Nogues, P., Massé, G., 2013. Sea surface temperature and sea ice variability in the subpolar North Atlantic from explosive volcanism of the late thirteenth century. Geophysical Research Letters 40, 5526-5530, doi: 10.1002/2013GL057282.

Simmonds, I., Li, M., 2021. Trends and variability in polar sea ice, global atmospheric circulations, and baroclinicity. Annals of the New York Academy of Sciences 1504, 167-186.

Smik, L., Cabedo-Sanz, P., Belt, S.T., 2016. Semi-quantitative estimates of paleo Arctic sea ice concentration based on source-specific highly branched isoprenoid alkenes: A further development of the PIP_{25} index. Organic Geochemistry 92, 63-69.

Steele, M., Ermold, W., Zhang, J., 2008. Arctic Ocean surface warming trends over the past 100 years. Geophysical Research Letters 35, L02614, doi: 10.1029/2007GL031651.

Stein, R., Fahl, K., Schade, I., Manerung, A., Wassmuth, S., Niessen, F., Nam, S.-I., 2017. Holocene variability in sea ice cover, primary production, and Pacific-Water inflow and climate change in the Chukchi and East Siberian Seas (Arctic Ocean). Journal of Quaternary Science 32, 362-379.

Stroeve, J., Notz, D., 2018. Changing state of Arctic sea ice across all seasons.

Environmental Research Letters 13, 103001.

Stroeve, J.C., Markus, T., Boisvert, L., Miller, J., Barrett, A., 2014. Changes in Arctic melt season and implications for sea ice loss. Geophysical Research Letters 41, 1216-1225, doi: 10.1002/2013GL058951.

Stroeve, J.C., Maslanik, J., Serreze, M.C., Rigor, I., Meier, W., Fowler, C., 2011. Sea ice response to an extreme negative phase of the Arctic Oscillation during winter 2009/2010. Geophysical Research Letters 38, L02502. http://dx.doi.org/10.1029/2010GL045662.

Su, L., Ren, J., Sicre, M.-A., Bai, Y., Jalali, B., Li, Z., Jin, H., Astakhov, A.S., Shi, X., Chen, J., 2022. HBIs and sterols in surface sediments across the East Siberian Sea: Implications for palaeo sea-ice reconstructions. Geochemistry, Geophysics, Geosystems 23, e2021GC009940. https://doi.org/10.1029/2021GC009940.

Thomas, D.N., 2017. Sea Ice, 3rd ed. John Wiley & Sons, Chichester.

Thompson, D. W. J., and Wallace, J. M., 1998: The Arctic oscillation signature in the wintertime geopotential height and temperature fields. Geophysical Research Letters 25, 1297–1300.

Walsh, J.E., Fetterer, F., Scott Stewart, J., Chapman, W.L., 2016. A database for depicting Arctic sea ice variations back to 1850. Geographical Review 107, 89-107.

Wang, J., Zhang, J., Watanabe, E., Ikeda, M., Mizobata, K., Walsh, J.E., Bai, X., Wu, B., 2009. Is the dipole anomaly a major driver to record lows in Arctic Summer sea ice extent? Geophysical Research Letters 36, L05706. http://dx.doi.org/10.1029/2008GL036706.

Wang, M., Overland, J.E., 2009. A sea ice free summer Arctic within 30 years? Geophysical Research Letters 36, L07502. http://dx.doi.org/10.1029/2009GL037820.

Wang, M., Overland, J.E., 2012. A sea ice free summer Arctic within 30 years: an update from CMIP5 models. Geophysical Research Letters 39, L18501. http://dx.doi.org/10.1029/2012GL0522868.

Wang, M., Yang, Q., Overland, J.E., Stabeno, P., 2018. Sea-ice cover timing in the Pacific Arctic: The present and projections to mid-century by selected CMIP5 models. Deep Sea Research Part II: Topical Studies in Oceanography 152, 22-34.

Wassmann, P., Duarte, C.M., Agusti, S., Sejr, M.K., 2011. Footprints of climate change in the Arctic marine ecosystem. Global Change Biology 17, 1235–1249.

Weingartner, T., Aagaard, K., Woodgate, R., Danielson, S., Sasaki, Y., Cavalieri, D., 2005. Circulation on the north central Chukchi Sea shelf. Deep Sea Research Part II: Topical Studies in Oceanography 52, 3150-3174.

Wendler, G., Chen, L. & Moore, B., 2014. Recent sea ice increase and temperature decrease in the Bering Sea area, Alaska. Theoretical and Applied Climatology 117, 393–398. https://doi.org/10.1007/s00704-013-1014-x.

Woodgate, R. A., & Peralta-Ferriz, C., 2021. Warming and freshening of the Pacific inflow to the Arctic from 1990-2019 implying dramatic shoaling in Pacific Winter Water ventilation of the Arctic water column. Geophysical Research Letters 48, e2021GL092528. https://doi.org/10.1029/2021GL092528.

Woodgate, R.A., 2018. Increases in the Pacific inflow to the Arctic from 1990 to 2015, and insights into seasonal trends and driving mechanisms from year-round Bering Strait mooring data. Progress in Oceanography 160, 124-154.

Yamamoto, M., Nam, S.I., Polyak, L., Kobayashi, D., Suzuki, K., Irino, T., Shimada, K., 2017. Holocene dynamics in the Bering Strait inflow to the Arctic and the Beaufort Gyre circulation based on sedimentary records from the Chukchi Sea. Climate of the Past 13, 1-50.

Yamamoto-Kawai, M., McLaughlin, F.A., Carmack, E.C., Nishino, S., Shimada, K.,

Kurita, N., 2009. Surface freshening of the Canada Basin, 2003–2007: River runoff versus sea ice meltwater. Journal of Geophysical Research: Oceans 114, C00A05, doi: 10.1029/2008JC005000.

Yang, X., Yuan, X., &Ting, M., 2016. Dynamical Link between the Barents-Kara Sea Ice and the Arctic Oscillation. Journal of Climate 29(14), 5103-5122.

Zhang, H., Xiao, X., 2021. Review of sea-ice reconstruction approach in the Arctic Ocean. Quaternary Sciences, 41, 813-823 (in Chinese with English abstract).

Zhuang, Y., Jin, H., Chen, J., Ren, J., Zhang, Y., Lan, M., Zhang, T., He, J., Tian, J., 2020. Phytoplankton Community Structure at Subsurface Chlorophyll Maxima on the Western Arctic Shelf: Patterns, Causes, and Ecological Importance. Journal of Geophysical Research: Biogeosciences 125, e2019JG005570.

Centennial-scale variability of sea-ice cover in the Chukchi Sea since AD 1850 based on biomarker reconstruction

Youcheng Bai *et al.*

Figures and captions

Figure 1-7

Figure 1

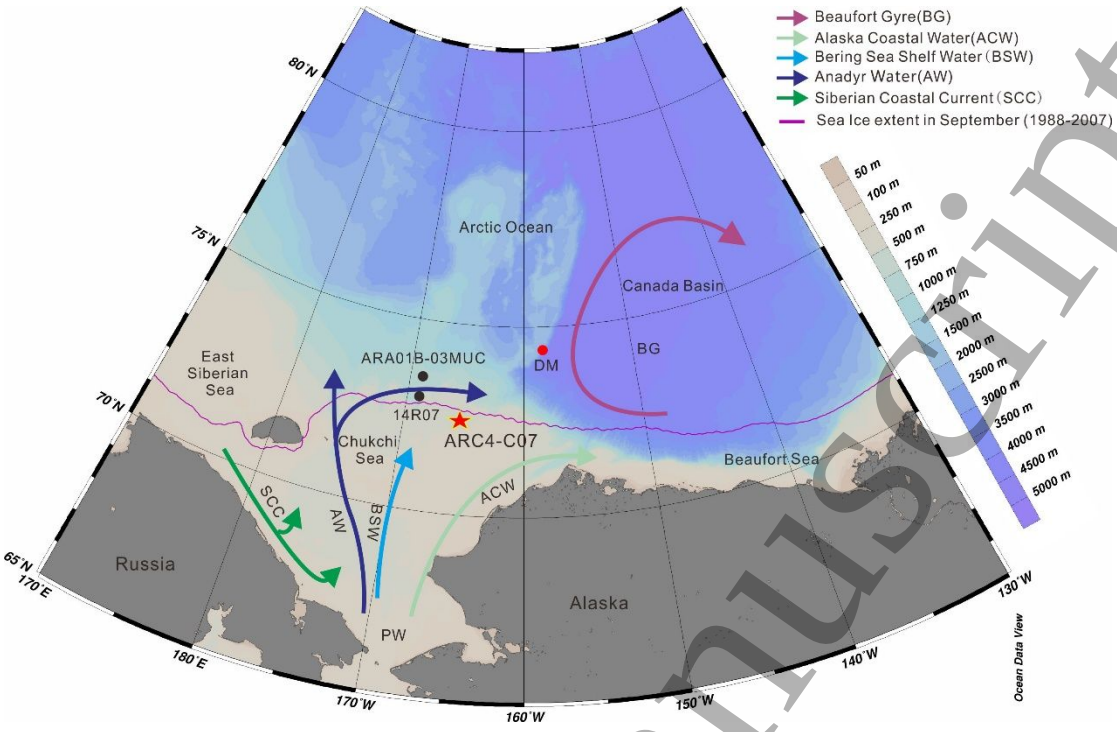

Figure 1. Map of the western Arctic Ocean and oceanographic setting (after Danielson et al., 2011). The red star indicates the locations of core ARC4-C07. The black dots show other sediment cores discussed in the text (Astakhov et al., 2019; Kim et al., 2019; more information can be found in Table S1). The red dot indicates the mooring site (Station DM) (Bai et al., 2019). The purple line features the mean September sea-ice extent for the 1988-2007 period (15% of sea ice concentration) (from Cavalieri et al., 1996, https://nsidc.org/). Current systems: PW-Pacific Water; SCC-Siberia Coastal Current; AW-Anadyr Water; BSW-Bering Shelf Water; ACW-Alaska Coastal Water; BG-Beaufort Gyre.

Figure 2

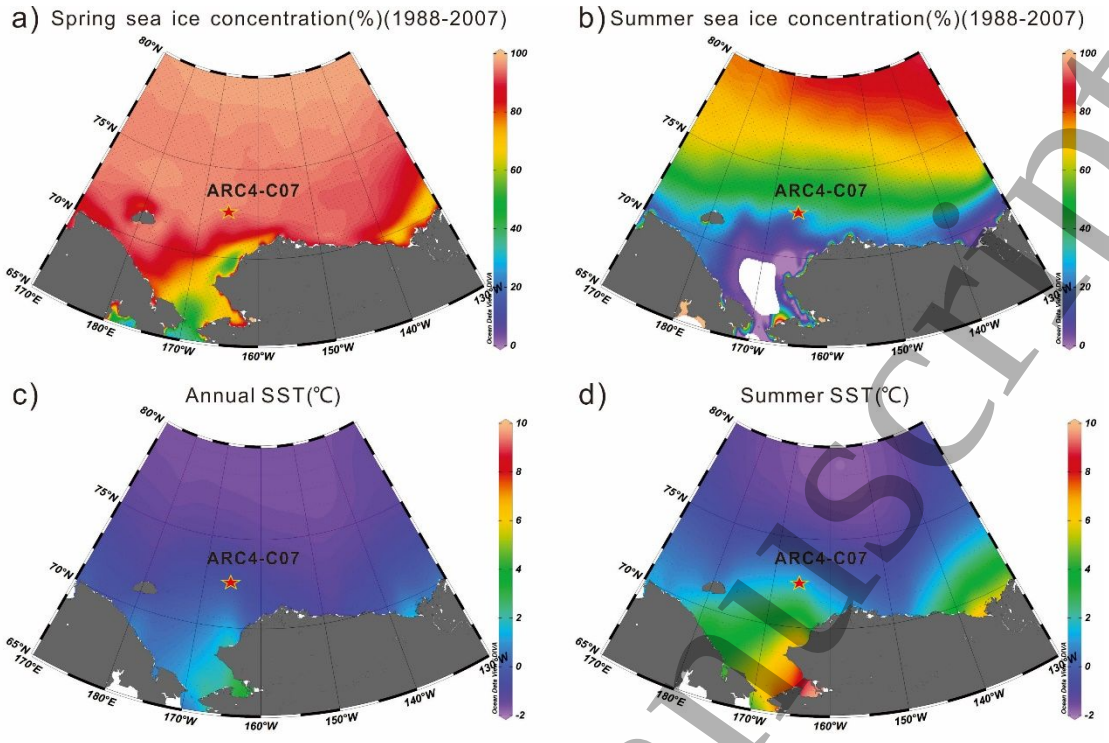

Figure 2. Averaged sea-ice concentrations from 1988-2007 for (a) spring (April, May and June) and (b) summer (July, August and September) (data source, http://nsidc.org). Averaged (c) annual Sea Surface Temperature (SST) and (d) summer SST (data source: Word Ocean Atlas 2013). The red star indicates location of core ARC4-C07.

Figure 3

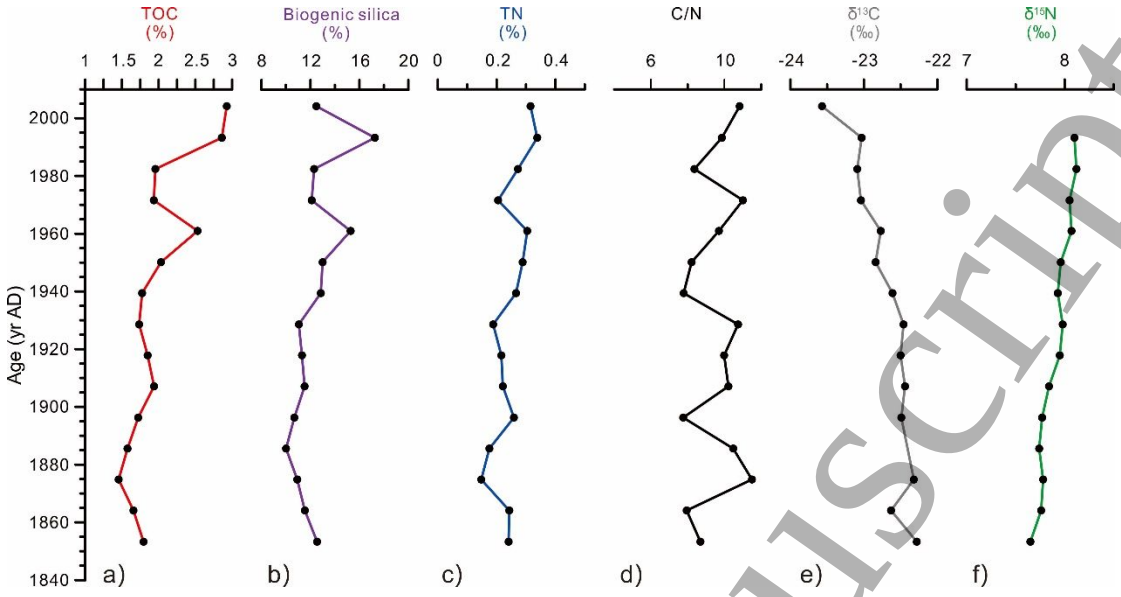

Figure 3. Downcore profiles of a) Total Organic Carbon, TOC in %; b) Biogenic silica in %; c) Total Nitrogen, TN in %; d) C/N ratio; e) carbon isotopic composition ($\delta^{13}C$) of the TOC in ‰ and f) nitrogen isotopic composition ($\delta^{15}N$) in ‰ from core ARC4-C07.

Figure 4

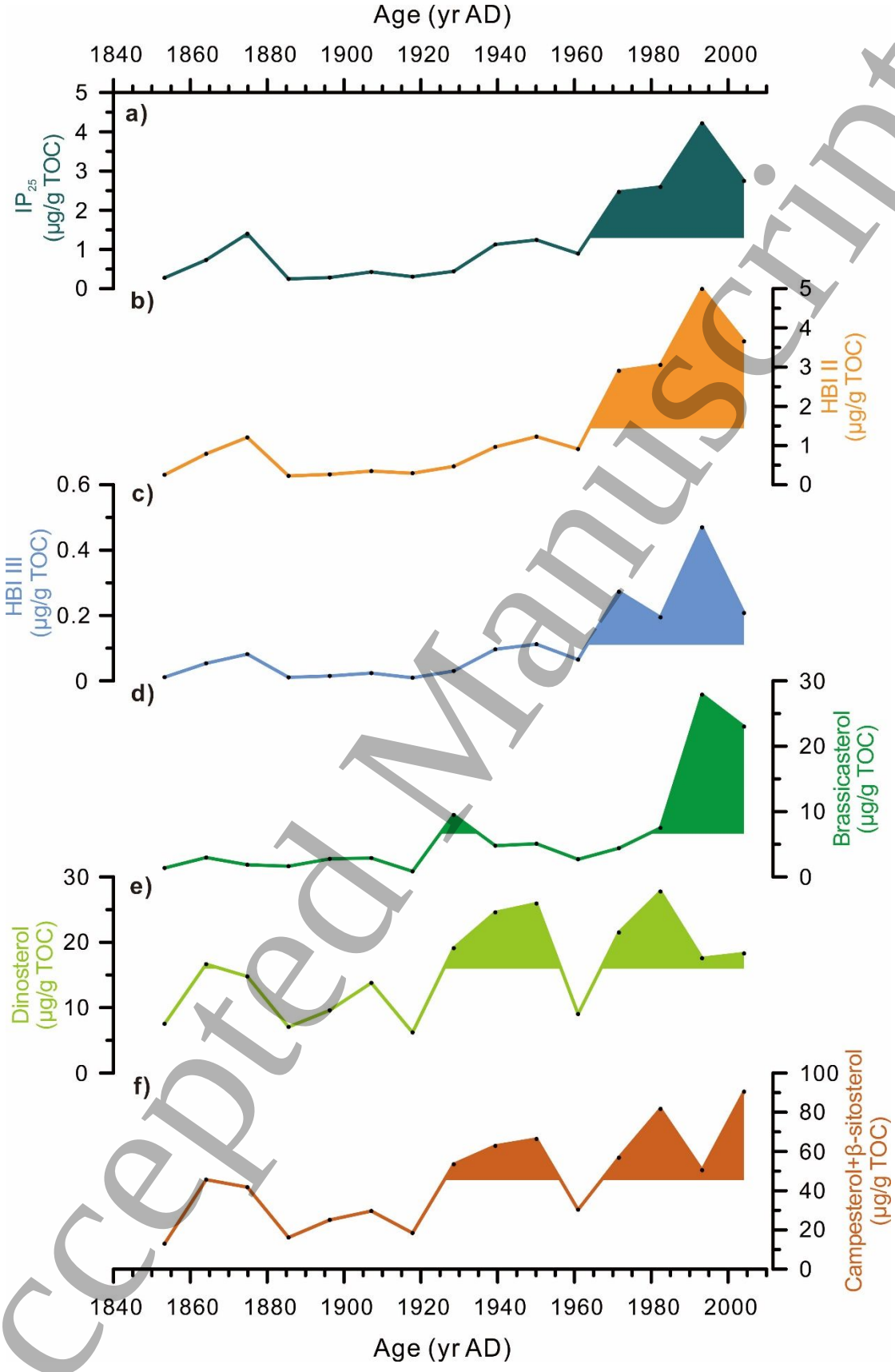

Figure 4. Biomarker concentrations in core ARC4-C07. a) Abundances relative to internal standard and normalized to TOC of IP_{25} in µg/g TOC; b) HBI II in µg/g TOC;

c) and HBI III in µg/g TOC; Concentrations normalized to TOC of d) Brassicasterol in µg/g TOC; e) Dinosterol in µg/g TOC; f) terrigenous sterols campesterol+β-sitosterol in µg/g TOC. Colored shading highlights values above the downcore mean.

Figure 5

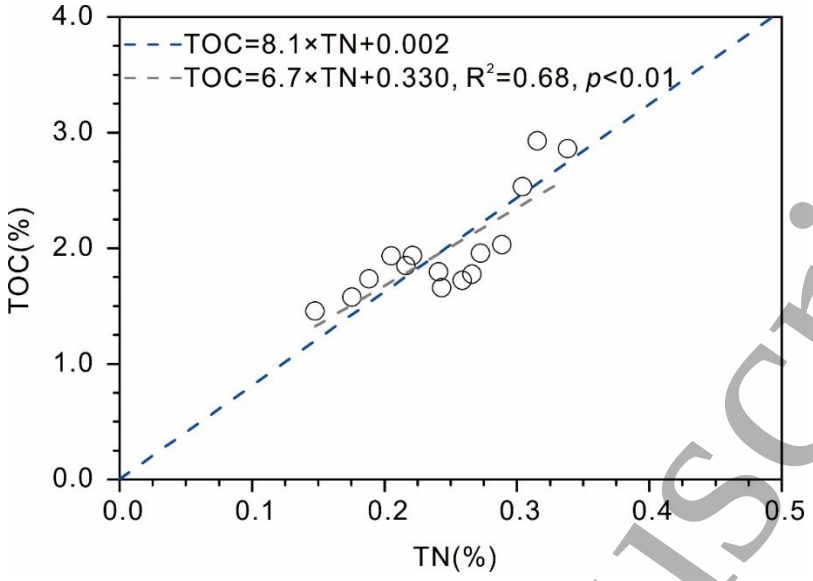

Figure 5. Cross-plot of downcore values of TOC (in %) and TN (in %) for core ARC4-C07 (in grey). The blue dashed line shows the linear from Goñi et al. (2013) derived from surface sediments across the North American Arctic margin and showing the slope of 8.1.

Figure 6

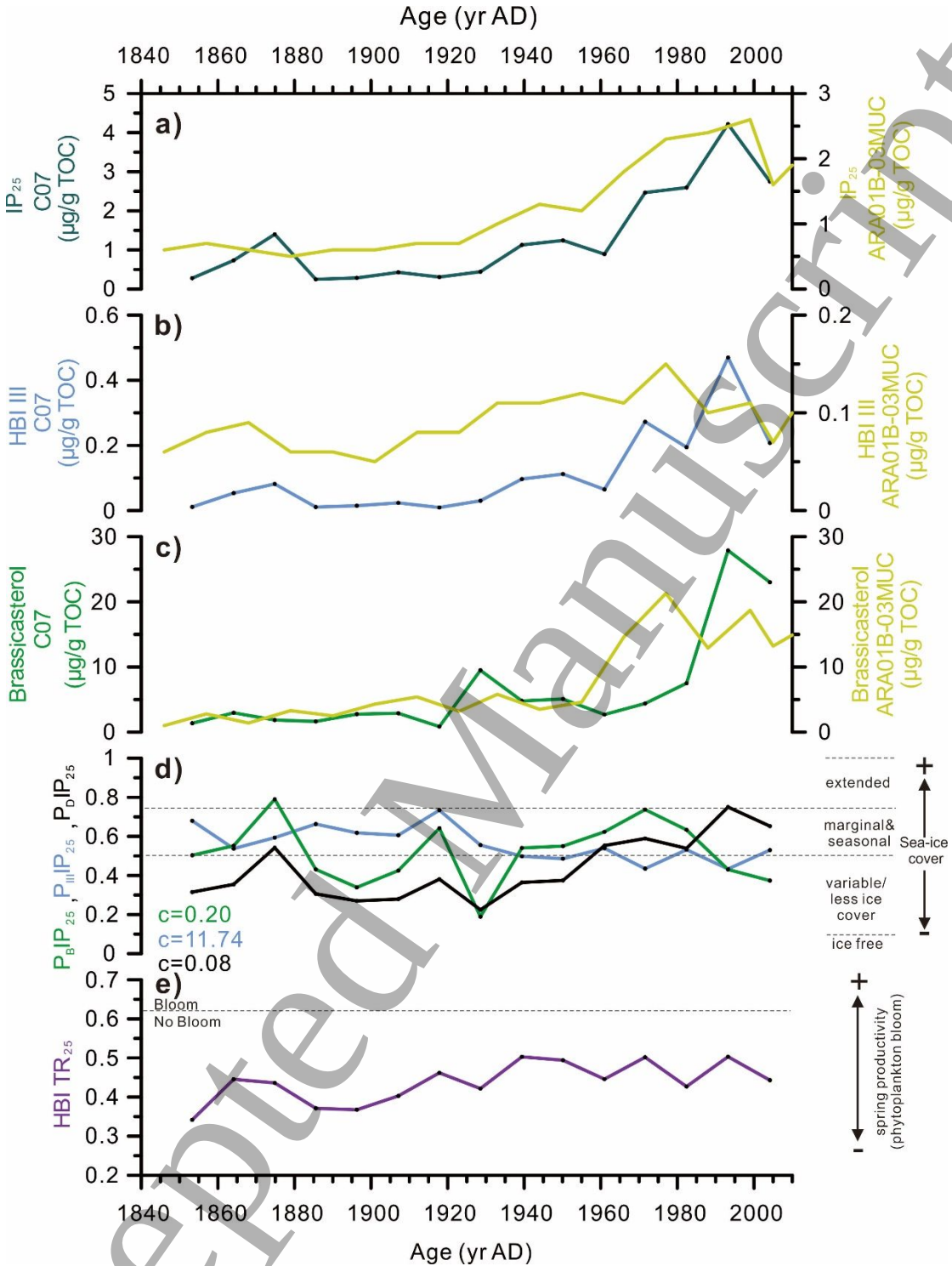

Figure 6. Downcore biomarker profiles of a) IP_{25}; b) HBI III; c) brassicasterol from core ARC4-C07; d) PIP_{25} index using brassicasterol (P_BIP_{25}, c=0.20 as calculated from the current core dataset), dinosterol (P_DIP_{25}, c=0.08 as calculated from the current core dataset), and HBI III ($P_{III}IP_{25}$, c=11.74 as calculated from the current core dataset); e) HBI TR_{25} calculated according to Belt et al. (2019). The dotted horizontal line ~0.62 indicates the threshold for the spring phytoplankton as established by Belt et al. (2019). The yellow lines show the IP_{25}, HBI III and brassicasterol measured in core ARA01B-

03MUC (Kim et al., 2019). Values can be found in Supplementary Table 2.

169 **Figure 7**

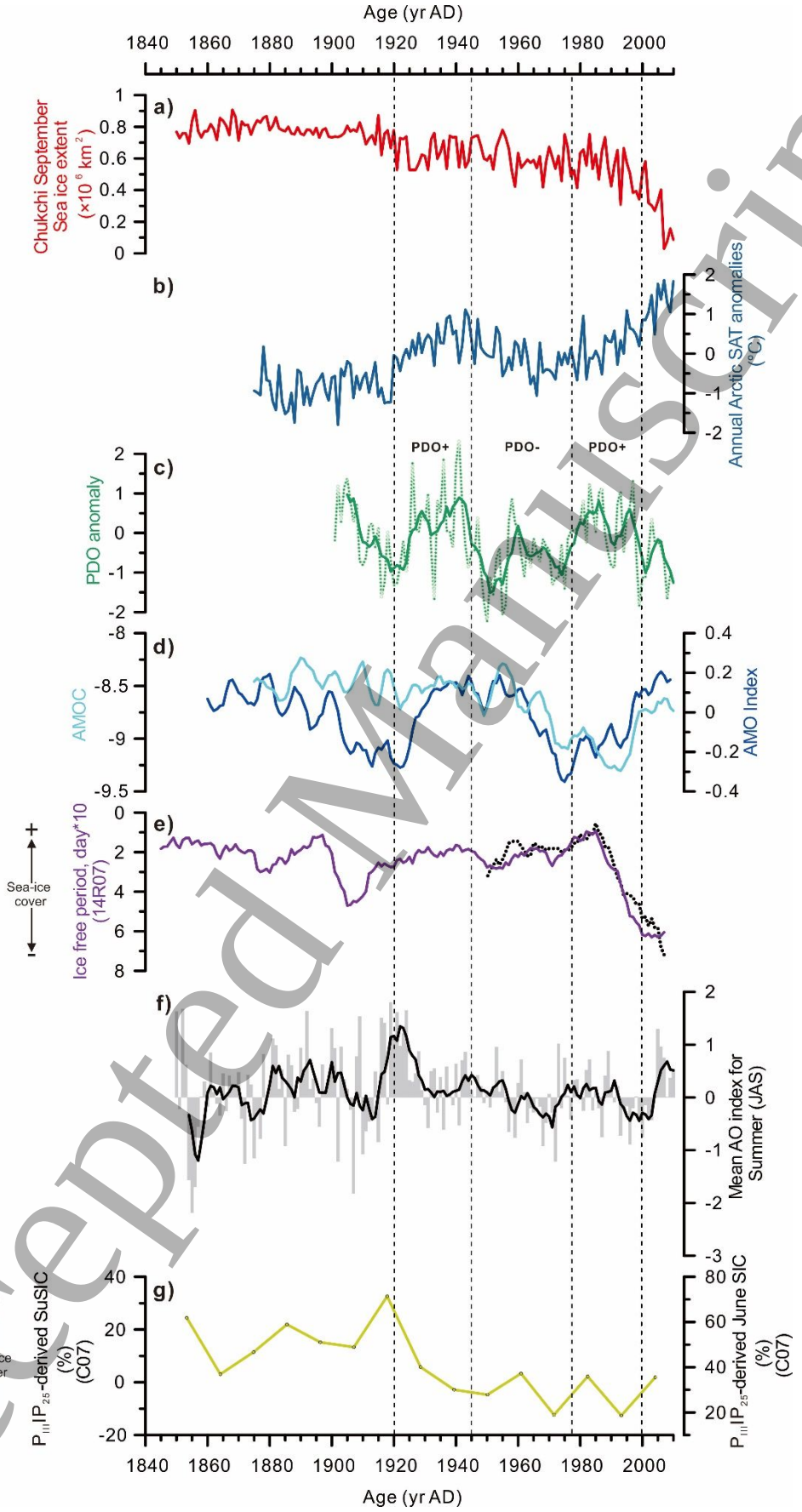

170

Figure 7. Comparison of $P_{III}IP_{25}$-derived summer sea ice (SuSIC) and June sea ice (June-SIC) of core ARC4-C07 with climatic and paleoceanographic records. a) September sea-ice extent record for the Chukchi Sea (Walsh et al., 2016); b) Composite time series of the annual Arctic surface air temperature (SAT) anomalies (℃) relative to 1961-90 Arctic temperature anomalies (Polyakov et al., 2002); c) Pacific Decadal Oscillation (PDO) Index (from Halfar et al., 2011); d) AMO (Atlantic Multidecadal Oscillation) Index (www.psl.noaa.gov/data/timeseries/AMO/) and AMOC (Atlantic Meridional Overturning Circulation) (from Caesar et al., 2018); e) Reconstruction of ice-free period at core 14R07 (in days). The black dotted line shows the observed duration of the ice-free period based on the elemental composition of sediments (from Astakhov et al., 2019); f) Arctic Oscillation (AO) mean index for summer (JAS)（Li and Wang, 2003); g) $P_{III}IP_{25}$-derived summer sea ice calculated using the relationship in Fig. S3a and for June-SIC using the relationship in Fig. S4a (see discussion). The bold lines in c and f represent the five-point running means. The vertical dashed lines indicate division of PDO phases as defined by Rodionov et al. (2007).